SYNTHESIS OF (1E, 1'E)-N, N'-(ETHANE-1, 2-DIYL) BIS (1-(4-(SUBSTITUTED) PHENYL)METHANIMINE) DERIVATIVE THEIR APPLICATION BIOLOGICAL AND DFT STUDIES

E. Enbaraj[1], H. Manikandan[1]*, D. Bhakiaraj[2]*

ArticleHistory:Received: 23/04/2023 Revised: 10/05/23 Accepted: 12/05/2023

Abstract

In the present work, two novel diamine-based benzyl dine were synthesized via a simple reaction. The structures of the resulting (1E,1'E)-N,N'-(ethane-1,2-diyl)bis(1-(4-(methylthio)phenyl)methanimine) (I) and (1E,1'E)-N,N'-(ethane-1,2-diyl)bis(1-(4-ethoxyphenyl)methanimine) (II) were established with the help of spectral-analytical techniques like; FTIR, ^{1}H, and ^{13}C NMR spectrometry. The compounds were further characterized by antibacterial with different pathogens. Compounds I and II were analyzed using Density Functional Theory (DFT) through the B3LYP method with 6-31G (d, p), as basis sets to determine HOMO-LUMO, Mulliken atomic charges, and molecular electrostatic potential (MEP) of compounds. The reactivity descriptors of B3LYP (EHOMO, ELUMO,) were calculated to predict the stability of newly synthesized compounds. The MEP analysis revealed that electronegative elements in the structure possess the maximum electronic cloud. The distributions of the various atoms were probed by Mulliken population analysis. The microbiological activity of the compounds was tested on several Gram-positive bacteria.

Keywords: Benzylidene, Spectral Analysis, Gram-Positive, HOMO-LUMO, MEP.

[1]Department of Chemistry, Annamalai University, Annamalainagar, Tamil Nadu - 608002, India.
[2]Department of Chemistry, St. Joseph's College of Arts and Science (Autonomous), Cuddalore, Tamil Nadu - 607001, India.
Corresponding Author: H.Manikandan, D. Bhakiaraj
Email: profmani.au@gmail.com, drdbr80@gmail.com

Doi: 10.48047/ecb/2023.12.5.104

Introduction

The azomethine group, which has a typical structure of RN=CH-R1 and may take on numerous substitutes, is what unites these substances structurally. Alkyl, aryl, cycloalkyl, and hetero molecules can all be represented by R and R1. Anils, imines, and azomethines among other names for these substances. Designing and creating novel chemical compounds with possible biological functions and fewer negative effects has drawn great interest from investigators, especially when it comes to creating Schiff bases for medicinal use [1-5]. Due to the ease with which they can be produced by fusion processes combining aldehydes and imines, schiff bases are known as "fortunate ligands" [6, 7]. Since Hugo Schiff coupled amine and carbonyl base compounds [8, 9] that had an azomethine (C=N-) functioning group, he first found Schiff bases. Since that time, Schiff bases have gained popularity as drugs for the synthesis of numerous substances with biological activity. The growth of such molecules' biological properties depends on the carbon-nitrogen double-bond unit [10, 11]. Due to the nitrogen particle's single pair of electrons, the double bond's electric charge-donating nature, and the nitrogen's weak electron attraction are biologically active [12–14] and can be used as antiradical, antimalarial, antiviral, cancer prevention, antimicrobial, antiseptic, and medication agents [15–17]. Certain complexes with donor N and O atoms have been developed as effective stereospecific catalysts for oxidative damage [18], reduction [19], hydration [20], enzyme activity [21, 22], and other chemical in nature and basic modifications.

These research served as the foundation for our decision to synthesize the compounds and test them for antibacterial activity. The products' IR, NMR, and mass spectrum data as well as DFT analyses were used to determine their structural assignments. The antibacterial activity of the substances mentioned in the title was examined.

Experimental

General

Sigma-Aldrich was the source of all the chemicals and solvents, which were all employed directly after acquisition. The changes in the mixture were watched using Thin Layer Chromatography (TLC) in sheets. The synthetic compounds have been characterized using multiple methods like FT-IR and NMR analyses. Using an Agilent Resolutions pro-FT-IR spectroscopy between 400 and 4000 cm-1, the wavelength range of FT-IR was measured. The proton and carbon-13 NMR spectra were recorded using a BRUKER 400 MHz NMR instrument with a solution consisting of as the most common solvent and TMS as an intramural background. The standard of reference was tetramethyl silane, and chemical shift readings were reported in parts per million (ppm).

Synthesis

Benzylidene derivatives: overall synthesis steps (I and II)

4-(methylthio) benzaldehyde/4-ethoxybenzaldehyde (2 mM), sodiumhydroxide (1 mM), and ethylenediamine (1 mM) in alcholic (25 mL) were used to create the benzylidene compounds, which were agitated for 8 hours at ambient temperature. Thin-layer chromatography was applied to analyse the end result of production (Scheme 1). After adding the outcome of the reaction mix to frigid water, the layer of precipitate that resulted was passed through filters and dehydrated. Through a series of recrystallization procedures using ethanol as a solvent, the compounds' purities consisted increased.

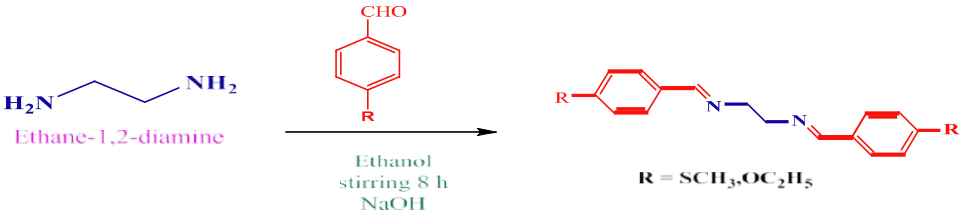

Scheme 1: Compound I and II's synthetic process Conditions and ingredients: 8 hours, room temperature, stirring, C2H5 OH, and NaOH.

(1E, 1'E)-N, N'-(ethane-1, 2-diyl) bis (1-(4-ethoxyphenyl) methanimine) (I)

Yield 92%; Greenish solid; 1H NMR (CDCl3, 400 MHz, ppm): δ 8.21 (s, 2H), 7.63 (d, 4H), 6.94 (d, 4H), 4.04 (m, 4H), 3.78 (s,4H), 7, 3.78 (t,6H), 7; 13C NMR (CDCl3, 100 MHz, ppm):δ 161.73, 160.90, 129.90, 129.15, 114.88, 63.69, 61.37, 14.99; IR (ATR) cm-1: 2982, 2934, 2886, 1680, 1596, 1475, 1394, 1250, 1037, 920, 827, 780.

(1E, 1'E)-N, N'-(ethane-1, 2-diyl) bis (1-(4-(methylthio) phenyl) methanimine) (I)

Yield 92%; Greenish solid; 1H NMR (CDCl3, 400 MHz, ppm): δ 8.26 (s, 2H),7.64 (d, 4H), 7.28 (d, 4H), 3.84 (s, 4H), 2.49 (s,6H); 13C NMR (CDCl3, 100 MHz, ppm):δ 161.76, 142.01, 133.04, 128.68, 125.86, 61.38, 14.48; IR (ATR) cm-1: 2986, 2920, 2826, 1689, 1586, 1434, 1387, 1300, 966, 807, 727.

Computational studies

The atomic arrangement of molecules I and II was built using a mixture of the functional B3LYP/6-31G (d, p) base set. The programme kit Gaussian 09W was used to perform the experiments. Bonding factors optimised the system at the best level of the concept, and the Gauss view approach was used to verify and present values for the HOMO-LUMO, Mulliken charges, and Meps [23–25].

Antibacterial activity

The developed compounds (I & II) were tested for their effectiveness as antibacterial agents against health care-associated bacterial pathogens utilizing the culture medium of agar well dissemination technique.

Results and discussion

FT-IR spectroscopy

The aromatic C-H bending frequencies for (I) and (II) were 2986 cm-1 and 2982 cm-1, correspondingly FT-IR (Figure 1). The noticeable bands about 2826 and 2920 cm-1 came about by the asymmetric extending bands of the -CH3 group and the symmetrical stretching bands of the -CH2 group for (I). Because the vibrations caused by stretching of the -CH3 and -CH2 groups for (II) were, in turn, asymmetric and symmetric, sharp bands could be seen at 2934 and 2886 cm-1. The average duration of the C-C, C=C stretch was 1434, 1586 cm-1 for (I) and 1475, 1596 cm-1 for (II).

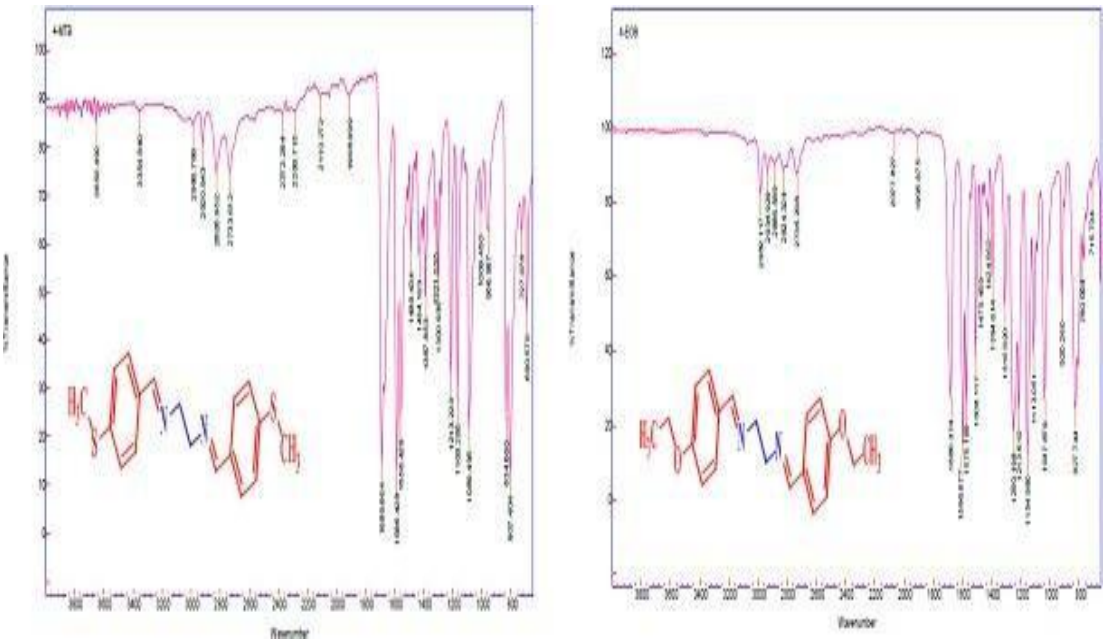

Figure 1: Compound (I&II)'s IR spectrum

The strong vibrations that stretch of (C=N) for (I) and (II) are detected at 1689 cm-1 and 1680 cm-1, respectively. The C-N stretched ratio was determined to be 1300 cm-1 for (I) and (II) and 1250 cm-1 for (II), accordingly. For -SCH3/-OC2H5, (I) and (II) have respective C-H bend rates of 1387 cm-1 and 1394 cm-1. The aromatic C-H bending ratios for -NCH2 were 807 cm-1 and 827 cm-1 for (I). Table 1 shows that the -CH2 rocking vibration are measured at 727 cm-1 for (I) and 780 cm-1 for (II).

Table 1: Compounds I and II in the IR spectrum determined at cm-1.

Assignments (cm^{-1})	**I**	**II**
ν (C-H)(Ar)	2986(w)	2982(s)
ν (C-H, a) of ($–SCH_3$/N-CH_2)/$–OC_2H_5$/N-CH_2)	2920(m)	2934(m)
ν (C-H, s) of ($–SCH_3$/N-CH_2)/$–OC_2H_5$/N-CH_2)	2826(m)	2886(W)
ν (C-O-C)	-	1037(s)
ν (C-C)	1434(m)	1475(m)
ν (C=C)	1586(s)	1596(s)
ν (C=N)	1689(m)	1680(m)
ν (C-N)	1300(s)	1250(s)
δ (C-H) of $–SCH_3$/$–OC_2H_5$	1387(m)	1394(m)
δ (C-H) of $–NCH_2$/ -NCH_2	966(s)	920(s)
δ (C-H)(Ar)	807(s)	827(m)
δ (CH_2) rocking	727(m)	780(m)

^{1}H and ^{13}C NMR spectroscopy

The protons of the methylene groups (H6–8) are allocated a singlet signal at 2.49 ppm in the compound's ^{1}H NMR spectrum, and the protons of H4 and H4' are assigned a doublet signal at 7.62 ppm. Aromatic H5 and H5' protons have a singlet signal attributed to them at 7.26 ppm, and aromatic H3 protons have a singlet sign given to them at 8.19 ppm. N-C-H protons (H1 and H2) are given a singlet signal with a wavelength of 3.84 ppm. The thiomethyl carbons C7 are visible at a frequency of 14.68 ppm in the compound. (I)'s ^{13}C NMR spectra. At 125.86 ppm, the C5 and C5' aromatic carbons were detectable. The aromatic carbons C4 and C4' also show up at 128.68 ppm. At 133.04 ppm, a C3 ipso carbon signal may be seen. There is a C6 carbon signal at 142.01 ppm. There are 161.76 and 61.38 ppm of C1 and C2 (C=N) carbons, respectively. The results of the compounds (I) and (II)'s 1H NMR spectra are displayed in Table 2 and Figure. 2.

Table 2: The ^{1}H and ^{13}C NMR's Compounds I and II spectral values

I		**II**	
Protons	**δ (ppm)**	**Protons**	**δ(ppm)**
$H_{1\&2}$	3.84	$H_{1\&2}$	3.78
H_3	8.26	H_3	8.21
$H_{5\&5'}$	7.26	$H_{5\&5'}$	6.92
$H_{4\&4'}$	7.62	$H_{4\&4'}$	7.60
$H_{6\text{-}8}$	2.49	$H_{6,7}$	4.02
-	-	$H_{8\text{-}10}$	1.31
Carbons	**δ(ppm)**	**Carbons**	**δ(ppm)**
C_1	61.38	C_1	61.37
C_2	161.76	C_2	160.90
C_3	133.04	C_3	129.15
C_6	142.01	C_6	161.73
$C_{4\&4'}$	128.68	$C_{4\&4'}$	129.15
$C_{5\&5'}$	125.86	$C_{5\&5'}$	114.88
C_7	14.68	C_7	63.69
-	-	C_8	14.99

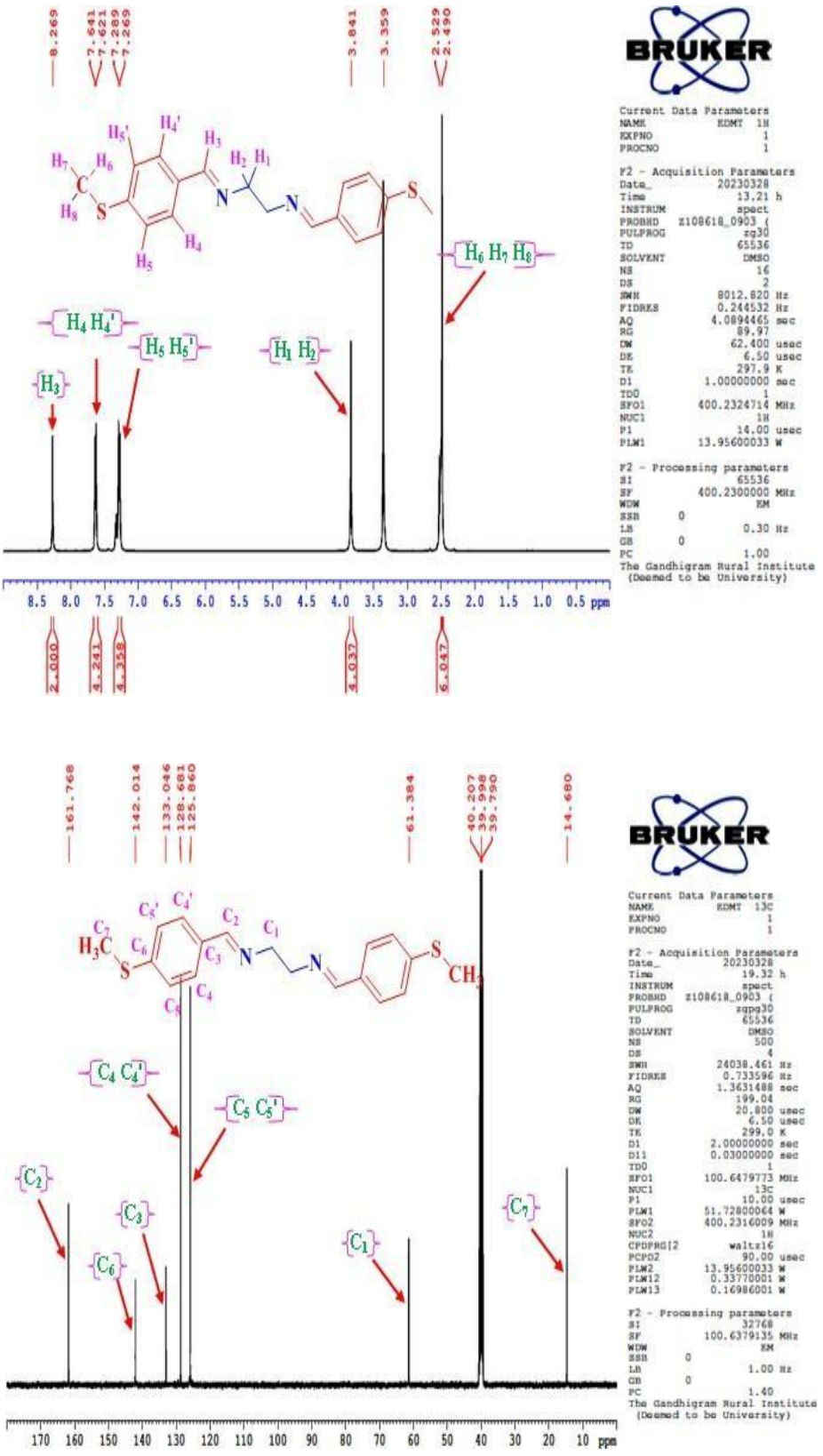

Figure 2: Compound (I)'s ^{1}H NMR and ^{13}C NMR spectra.

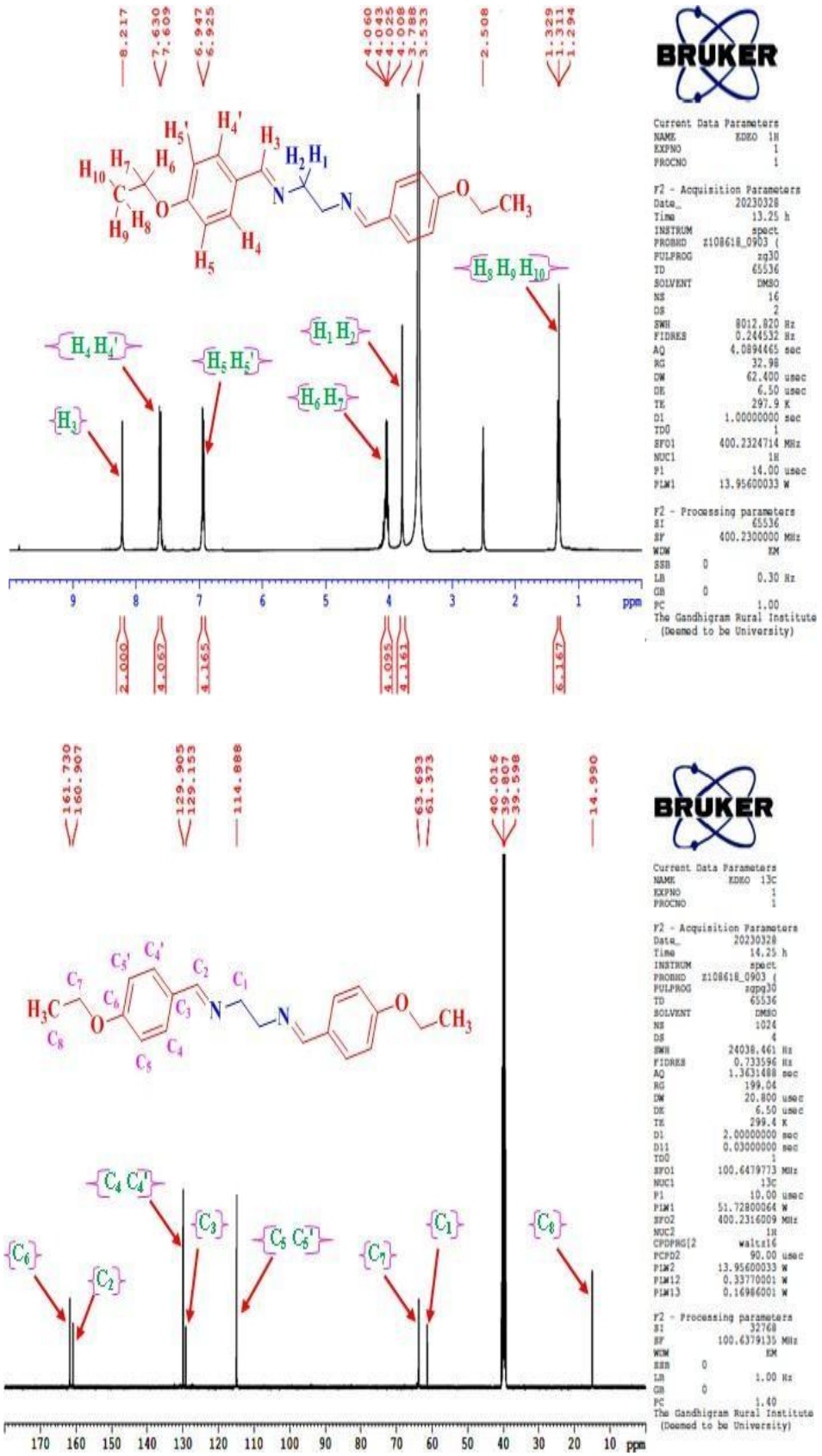

Figure 3: Compound (II) ^{1}H and ^{13}C NMR spectra

The protons of the CH3 groups (H8–10) are characterised by a triplet signal at 1.31 ppm in the ^{1}H-NMR spectra for compound (II) (Figure 3), while the protons of H4 and H4' are characterised by a doublet signal at 7.60 ppm. Aromatic H5 and H5' protons have a doublet signal assigned to them at 6.92 ppm, while aromatic H3 protons have a singlet signal at 8.21 ppm. N-C-H protons (H1 and H2) are given a singlet signal with a wavelength of 3.78 ppm. -OCH2 protons (H6, 7) were allocated to one quartet signal at 4.02 ppm. The CH3 carbons C8 are seen at a concentration of 14.99 ppm in the compound (II)'s ^{13}C NMR spectra. At 129.15 ppm, the C4 and C4' aromatic carbons were present. Similarly, at 114.88 ppm, the C5 and C5' aromatic carbons can be found. At 129.15 ppm, the C3 ipso carbon signal is visible. At 161.73 ppm, the C6 ipso carbon signal may be seen. There are 160.90 and 61.37 ppm worth of C1 and C2 (C=N) carbons, respectively. At 63.69 ppm, the CH2 carbons C7 are visible. Compounds (I) and (II)'s ^{1}H and ^{13}C NMR spectrum values are displayed in Table 2.

DFT Studies

Frontier molecular orbital analysis (FMO)

The additional species along the route with chemical interactions are called the Frontier Molecular Orbitals (LUMO and HOMO), and they are [27]. The FMO length describes both the chemical compound's kinetic stability and chemical responsiveness. A soft molecule is one that is more polarizable, more frequently linked to greater chemical responsiveness, less kinetic predictability, and a constrained planetary limit gap. The HOMO and LUMO serve as electron donors and acceptors, respectively, while operating as orbitals. Figure 4 displays the I&II LUMO plots and 3D HOMO FMO plots. In compounds I and II, the HOMO is located in the thio methyl group and phenyl rings, respectively. For technological uses, Molecules I and II will be preferable to the stack-transfer connection that ends in Table 3.

Table 3: B3LYP/6-31G (d, p)'s calculations of the HOMO-LUMO energies and quantum chemical parameter values.

Property	**Compounds**	
B3LYP/6-31G(d,p)	**I**	**II**
E_{HOMO}	-6.4575	-5.9459
E_{LUOMO}	-0.5586	-1.1181
$E_{LUMO-HOMO}$	5.8989	4.8279
Electronegativity(χ)	-3.5081	-3.5319
Hardness(η)	2.9494	2.4139
Electrophilicity index (Ψ)	2.0862	2.5839
Softness(ξ)	0.1695	0.2071

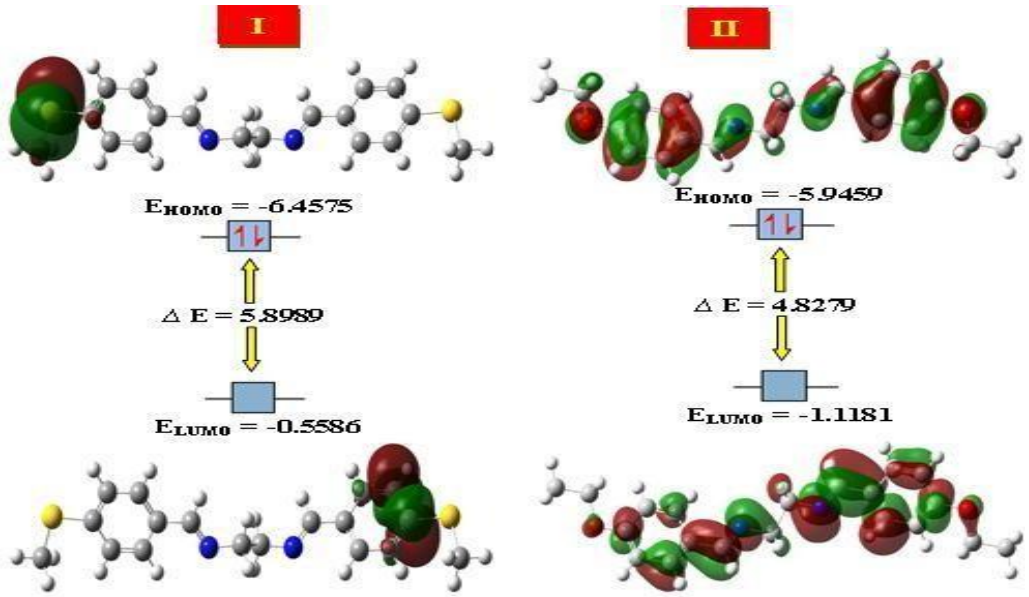

Figure.4 Frontier molecular orbital of compound (I&II).

Mulliken population analysis

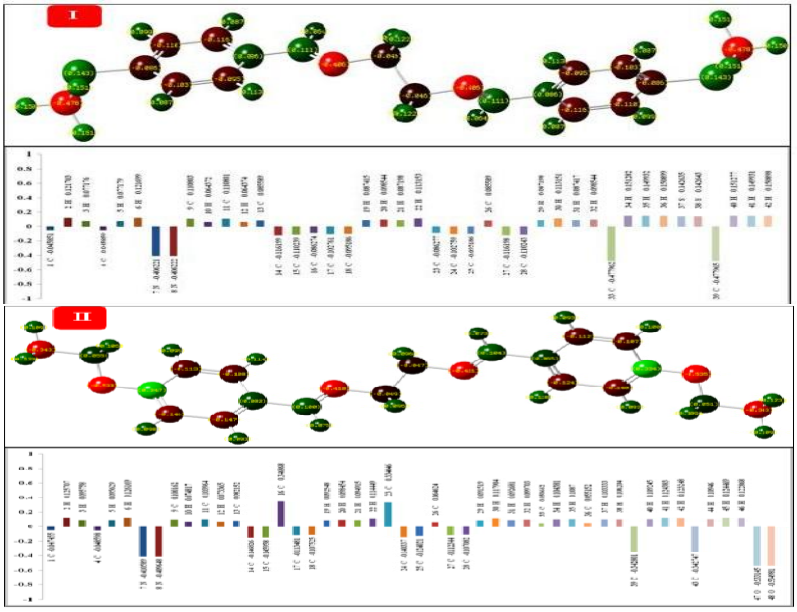

Figure 5: Mulliken atomic charge distribution and Mulliken plot of compounds (I) & (II)

Table 4: Mulliken charges of (I) and (II)

Compound I				**Compound II**			
Atom	Charges	Atom	Charges	Atom	Charges	Atom	Charges
1C	-0.04585	22H	0.113153	1C	-0.04746	25C	-0.12402
2H	0.121703	23C	-0.08628	2H	0.125707	26C	0.064624
3H	0.077176	24C	-0.10276	3H	0.095758	27C	-0.11234
4C	-0.04586	25C	-0.09519	4C	-0.0486	28C	-0.10708
5H	0.077179	26C	0.085589	5H	0.095629	29H	0.091519
6H	0.121699	27C	-0.1162	6H	0.126169	30H	0.117904
7N	-0.40622	28C	-0.11024	7N	-0.41059	31H	0.092681
8N	-0.40622	29H	0.087198	8N	-0.40965	32H	0.099703
9C	0.110803	30H	0.113151	9C	0.100162	33C	0.050662
10H	0.064372	31H	0.087417	10H	0.074817	34H	0.104381
11C	0.110801	32H	0.098544	11C	0.103964	35H	0.1087
12H	0.064374	33C	-0.47796	12H	0.073365	36C	0.055152
13C	0.085589	34H	0.151282	13C	0.082152	37H	0.103333
14C	-0.1162	35H	0.149932	14C	-0.14683	38H	0.106204
15C	-0.11024	36H	0.150899	15C	-0.14596	39C	-0.3428
16C	-0.08627	37S	0.142635	16C	0.346868	40H	0.109245
17C	-0.10276	38S	0.142643	17C	-0.11348	41H	0.124383
18C	-0.09519	39C	-0.47797	18C	-0.10753	42H	0.123248
19H	0.087415	40H	0.151277	19H	0.092548	43C	-0.34275
20H	0.098544	41H	0.149931	20H	0.098454	44H	0.10946
21H	0.087198	42H	0.150898	21H	0.094915	45H	0.124469
-	-	-	-	22H	0.114449	46H	0.122868
-	-	-	-	23C	0.334046	47O	-0.53315
-	-	-	-	24C	-0.14034	48O	-0.53498

The determination of valuable atomic charge is crucial in the application of quantum mechanical calculations to molecular systems [28]. The Mulliken atomic charges are determined using the base characteristic electron population of each atom. The charge distribution and plot of (I) are shown in Figure 5. From the atomic charge values the nitrogen (N7 and N8) and carbon (C1, C4, C14, C15, C16, C17, C18, C23, C24, C25, C27, C29, C33, and C39) in the compound for (I) had a large negative charge and behaved as electron donors. Similarly, oxygen (O47 and O48), nitrogen (N7 and N8) and carbon (C1, C4, C14, C15, C17, C18, C25, C27, C28, C39 and C43) in the compound for (II) exhibited a strong negative charge and electron donor behaviour. The remaining atoms (all H atoms C9, C11, C13, C26 and S37, S38 (I)) and (all H atoms C9, C11, C13, C16, C23, C26, C33 and C36 (II)) are acceptors exhibiting positive charge. The negative charges on nitrogen/oxygen, which is a donor atom and the net positive charge on the hydrogen atom, which is an acceptor atom suggest the presence of intra- and intermolecular hydrogen bonding interactions. The Mulliken charge population values are given in Table 4.

Molecular electrostatic potential

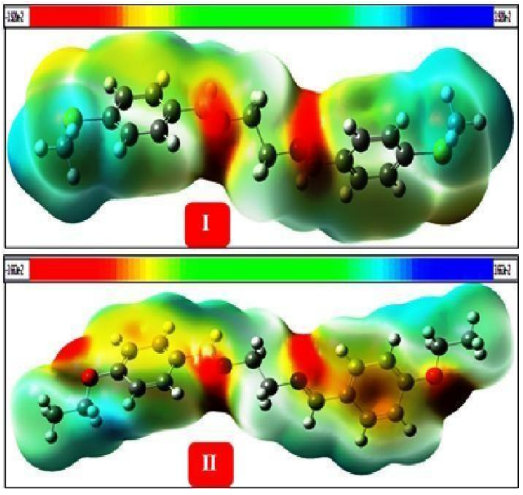

Figure 6: Molecular electrostatic potential of compound (I&II).

The electronegativity, partial charges, and chemical reactivity of a molecule are all correlated with its molecular electrostatic potential (MEP), which measures the net electrostatic impact created at a specific location by the entire charge distribution of the atom or molecule. MEP is a well-known, effective approach for explaining and foretelling molecular reactive activity. The different values of the electrostatic potential at the surface are represented by different colours. Potential increases in the order of red < orange < yellow < green < blue. The colour code of these maps is in the range between −3.920 × 10−2 (deepest red) to +3.920 × 10−2 (deepest blue) for (I) and-3.663 × 10−2 (deepest red) to +3.663 × 10−2 (deepest blue) for (II), more electronegativity appears at the oxygen and nitrogen atoms indicated by yellow colour. The zone of bright green that dominates the MEP's surface might be thought of as a potential midpoint between the extremes of red and dark blue colours. The positive sections were connected to nucleophilic reactivity, while the negative regions were connected to electrophilic reactivity. The areas around the oxygen and nitrogen atoms in compounds (I) and (II) have negative potential, as can be shown in Figure.6. The electrophiles tend to the negative and the nucleophiles tend to the region of positive MEP. Molecular surfaces obtained by B3LYP level 6–31 G (d, p) as the basis set [29].

The diffusion technique using agar wells for testing antibacterial activit

The compound I screened for antibacterial activity against four bacterial pathogens (table 5&6) (Figure. 7). In antibacterial assay, the compound I showed the maximum zone of inhibition observed in Escherichia coli (23 ±1.53 mm) followed by Streptococcus pneumoniae (20 ±1.00) , Klebsiella pneumoniae (20 ±1.00) and minimum zone of inhibition observed in Staphylococcus aureus (14 ±0.58mm) at 100 µl concentration. The compound II screened for antibacterial activity against four bacterial pathogens.

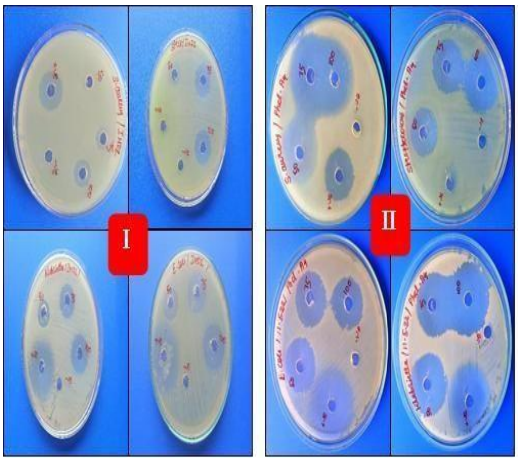

Figure: 7 Antibacterial activity of compound (I &II)

Table 6. Antibacterial Activity against Four Bacterial Pathogens of Compound I

S.NO	Bacterial Pathogens	Zone Of Inhibition (mm)				
		I				
		50 µl	75 µl	100 µl	Positive control	Negative Control
1	*Staphylococcus aureus*	10±1.00	12 ±1.00	14 ±0.58	19 ±1.53	-
2	*Streptococcus pneumoniae*	14 ±0.58	19 ±0.58	20 ±1.00	24 ±1.00	-
3	*Escherichia coli*	17 ±1.53	21 ±0.58	23 ±1.53	28 ±0.58	-
4	*Klebsiella pneumoniae*	14 ±1.53	18 ±1.53	20 ±1.00	31 ±0.58	-

Table 6. Antibacterial Activity against Four Bacterial Pathogens of Compound II

S.NO	Bacterial Pathogens	Zone Of Inhibition (mm)				
		II				
		50 µl	75 µl	100 µl	Positive control	Negative Control
1	*Staphylococcus aureus*	26 ±1.00	28±1.00	29 ±0.58	30 ±0.58	-
2	*Streptococcus pneumoniae*	22 ±0.58	24 ±0.58	27 ±1.00	18 ±1.53	-
3	*Escherichia coli*	25 ±1.53	28 ±1.00	30 ±0.58	30 ±1.53	-
4	*Klebsiella pneumoniae*	28 ±1.00	30 ±1.53	32 ±1.00	30 ±1.00	-

In antibacterial assay, the compound I showed the maximum zone of inhibition observed in Klebsiella pneumoniae (32 ±1.00 mm) followed by Escherichia coli (30 ±0.58 mm) , Staphylococcus aureus (29 ±0.58 mm) and minimum zone of inhibition observed in Streptococcus pneumoniae (27 ±1.00 mm) at 100 µl concentration. Compare with both compounds better antibacterial activity showed in compound II against all the tested bacterial pathogens [30].

Conclusion

Finally, a novel (1E,1'E)-N,N'-(ethane-1,2-diyl)bis(1-(4-(substituted)phenyl)methanimine) (I & II) was created, and their structural integrity was verified using 1H and 13C NMR spectroscopy. Better antibacterial activity than the parent compound is present in the synthesized compounds. The activity of all the synthesized compounds versus pathogenic bacteria ranges from modest to excellent. Compounds I and II have more antibacterial potency than ciprofloxacin, whereas other compounds were roughly equal in strength. On compounds I and II, a DFT comparison study has been conducted. The stretching frequency of the IR spectra of compounds that were calculated theoretically and empirically show a strong relationship. The compounds were identified as descriptors of the measured chemical reactivity using the DFT experiments.

Credit Authorship Contribution Statement

E. Enbaraj: Conceptualization, Methodology, Software, Writing - original draft. H. Manikandan: Supervision, Writing - review & editing. D. Bhakiaraj: Supervision, Writing - review & editing. J.

Declaration of Competing Interest

The authors declare that they have no known competing financial interests or personal relationships that could have appeared to influence the work reported in this paper.

References

[1] A. Kajal, S. Bala, S. Kamboj, N. Sharma, V. Saini, J. Catal. "Schiff Bases: A Versatile Pharmacophore" (2013).

[2] Cimerman, Zvjezdana, Snežana Miljanić, and Nives Galić. "Schiff bases derived fromaminopyridines as spectrofluorimetric

analytical reagents." Croatica Chemica Acta 73.1 (2000): 81-95.

[3] Mohr, J.Gerhard, et al. "Development of chromogenic copolymers for optical detection of amines." Advanced Materials 10.16 (1998): 1353-1357.

[4] P.R. Patel, B.T. Thaker and S. Zele, "Preparation and characterisation of some lanthanide complexes involving a heterocyclic β– diketone." Indian J. Chem, 38 (1999) 563- 569.

[5] R.W. Layer, Chem. Rev., Washington, DC, U.K,63, (1963) 489-510.

[6] T.P. Yoon, E.N. Jacobsen, "Privileged ChiralCatalysts", Science 299, (2003) 1691

[7] P.G. Cozzi, "Metal–Salen Schiff base complexes in catalysis: practical aspects." Chem. Soc. Rev. 33, (2004) 410

[8] H. Schiff, H. Schiff, "Mittheilungen aus dem Universitätslaboratorium in Pisa: eine neue Reihe organischer Basen." Justus Liebigs Annalen der Chemie 131, (1864) 118.

[9] I.P. Ejidike, P.A. Ajibade, "Synthesis, characterization and biological studies of metal (II) complexes of (3 E)-3-[(2-{(E)-[1-(2, 4-dihydroxyphenyl) ethylidene] amino} ethyl) imino]-1-phenylbutan-1-one Schiff base." Molecules 20, (2015) 9788.

[10] A.O. De Souza, F.C.S. Galetti, C.L. Silva, B. Bicalho, M.M. Parma, S.F. Fonseca, "Antimycobacterial and cytotoxicity activity of synthetic and natural compounds." Quim. Nova 30, (2007) 1563

[11] Z. Guo, R. Xing, S. Liu, Z. Zhong, X. Ji, L. Wang, "Antifungal properties of Schiff bases of chitosan, N-substituted chitosan and quaternized chitosan." Carbohydr. Res. 342, (2007) 1329

[12] I. Kostova, L. Saso, "Advances in research of Schiff-base metal complexes as potent antioxidants." Curr. Med. Chem. 20, (2013) 4609

[13] D.N. Dhar, C.L. Taploo, "Schiff-bases and their applications." J. Sci. Ind. Res. 41, (1982) 501.

[14] C.M. Da Silva, D.L. Da Silva, L.V. Modolo, R.B. Alves, M.A. De Resende, C.V.B. Martins, A. de Fatima, J. Adv. Res. 2, (2011) 1

[15] P. Przybylski, A. Huczynski, K. Pyta, B. Brzezinski, F. Bartl, Curr. Org. Chem. 13, (2009) 124

[16] B. Halliwell, J.M.C. Gutteridge, 3rd edn. (Oxford University Press, New York, (1999).

[17] P. Arulpriya, P. Lalitha, S. Hemalatha, "Antimicrobial testing of the extracts of Samanea saman (Jacq.) Merr." Der Chemica Sinica 1, (2010) 73.

[18] R. I Kureshy, N.H. Khan, S.H.R. Abdi, S.T. Patel and P.J. Iyer, "Chiral Ru (II) Schiff base complex-catalysed enantioselective epoxidation of styrene derivatives using iodosyl benzene as oxidant. II." J. Mol. Catal. A: Chem, 150, (1999) 175-183.

[19] Y. Aoyama, J.T. Kujisawa, T. Walanawe, A. Toi and H. Ogashi, "Catalytic reactions of metalloporphyrins. 1. Catalytic modification of borane reduction of ketone with rhodium (III) porphyrin as catalyst." J. Am. Chem. Soc, 108, (1986) 943-947.

[20] T.R. Kelly, A. Whiting, and N.S. Chandra Kumar, "Rationally designed, chiral Lewis acid for the asymmetric induction of some Diels-Alder reactions." J. Am. Chem. Soc, 108, (1986) 3510-3512.

[21] P. Sengupta, S. Ghosh and T.C.W. Mak, "A new route for the synthesis of bis (pyridine dicarboxylato) bis (triphenylphosphine) complexes of ruthenium (II) and X-ray structural characterisation of the biologically active trans-[Ru (PPh3) 2 (L1H) 2](L1H2= pyridine 2, 3- dicarboxylic acid)." Polyhedron, 20, (2001) 975-980.

[22] A.S. Ramasubramanian, B.B. Ramachandra and R. Dileep, Synth. React. Inorg. Met. Org., Nano-Met.Chem, 42, (2012) 548-553.

[23] M.J. Frisch, G.W. Trucks, H.B. Schlegel, G.E. Scuseria, M.A. Robb, J.R. Cheeseman,G. Scalmani, V. Barone, G.A. Petersson, H. Nakatsuji, X. Li, M. Caricato, A.Marenich, J. Bloino, B.G. Janesko, R. Gomperts, B. Mennucci, H.P. Hratchian, J.V.Ortiz, A.F. Izmaylov, J.L. Sonnenberg, D. Williams- Young, F. Ding, F. Lipparini, F.Egidi, J. Goings, B. Peng, A. Petrone, T. Henderson, D. Ranasinghe, V.G. Zakrzewski,J. Gao, N. Rega, G. Zheng, W. Liang, M. Hada, M. Ehara, K. Toyota, R. Fukuda, J.Hasegawa, M. Ishida, T. Nakajima, Y. Honda, O. Kitao, H. Nakai, T. Vreven, K.Throssell, J.A. Montgomery, Jr., J. E. Peralta, F. Ogliaro, M. Bearpark, J.J. Heyd, E.Brothers, K.N. Kudin, V.N. Staroverov, T. Keith, R. Kobayashi, J. Normand, K.Raghavachari, A. Rendell, J.C. Burant, S.S. Iyengar, J. Tomasi, M. Cossi, J.M. Millam,M. Klene, C. Adamo, R. Cammi, J.W. Ochterski, R.L. Martin, K.

Morokuma, O.Farkas, J.B. Foresman, D.J. Fox, Gaussian, Inc., Wallingford CT, 2016.

[24] R. Dennington, T. Keith, J. Millam, Gauss View, Version 5. Semichem Inc., ShawneeMission (2009).

[25] M.A. Spackman, D. Jayatilaka, Hirshfeld surface analysis, Cryst. Eng. Commun. 11 (2009) 19-32.

[26] Y. Bouzian, Y. Sert, K. Khalid, L. V. Meervelt, K. Chkirate, L. Mahi, N. H. Ahabchane,
A. Talbaoui, E. M. Essassi. J. Mol. Struct., 1246, (2021)131217.

[27] S. Gunasekaran, S. Kumaresan, R. Arunbalaji, G. Anand, S. Srinivasan, Density functional theory study of vibrational spectra, and assignment of fundamental modes of dacarbazine, J. Chem. Sci. 120 (2008) 315–324.

[28] S. Gunasekaran, S. Kumaresan, R. Arunbalaji, G. Anand, S. Srinivasan, J. Chem. Sci.,120, (2008) 315–324.

[29] V. Meenatchi, R. Agilandeshwari and S.P. Meenakshisundaram. RSC Adv., 5, (2015) 71076–71087.

[30] J. Vigneshwari, et al. "Broad spectrum of bioactive compounds from halophilic actinomycetes isolated from the Kodiyakadu saltpan of Vedaranyam-India." Materials Today: Proceedings 59 (2022): 979-987.